

pH-induced size changes in solutions of cholesteric liquid- crystal polymers studied by SANS

This content has been downloaded from IOPscience. Please scroll down to see the full text.

2014 J. Phys.: Conf. Ser. 554 012011

(<http://iopscience.iop.org/1742-6596/554/1/012011>)

View [the table of contents for this issue](#), or go to the [journal homepage](#) for more

Download details:

IP Address: 161.111.65.60

This content was downloaded on 11/11/2014 at 10:28

Please note that [terms and conditions apply](#).

pH-induced size changes in solutions of cholesteric liquid-crystal polymers studied by SANS

Mercedes Pérez Méndez¹, Daniel Rodríguez Martínez^{2,3} and Stephen M King³.

¹ Institute of Polymer Science and Technology, Group of Physical-Chemistry and Modelization of Macromolecules (PCMM), C/ Juan de la Cierva, 3. 28006 Madrid, Spain

² Retinal degeneration: from genetics to therapy Laboratory, Centro Andaluz de Biología Molecular y Medicina Regenerativa Edif. CABIMER Avda. Américo Vespucio, s/n Parque Científico y Tecnológico Cartuja 93. 41092 Sevilla, Spain

³ ISIS Facility, STFC Rutherford Appleton Laboratory, Harwell Oxford, Didcot, Oxfordshire OX11 0QX, United Kingdom

E-mail: perezmendez@ictp.csic.es

Abstract. Polycations possessing substantial buffering capacity below physiological pH, are intrinsically efficient transfection agents. These vectors have been shown to deliver genes as well as oligonucleotides, both *in vitro* and *in vivo*, by protecting DNA from inactivation by blood components. Their efficiency relies on extensive endosome swelling and rupture that provides an escape mechanism for the polycation/DNA complexes. Recently, biocompatible cationic cholesteric liquid-crystal polymers (ChLCP) have proved able to condense and successfully transfect DNA, acting as non-viral vectors. Here the radius of gyration of the new ChLCPs is determined by SANS as a function of pH, the ultimate aim being to correlate changes in polymer conformation with membrane activity. With increasing pH the polymers apparent radii of gyration increased to a maximum, before subsequently decreasing. This molecular expansion, on passing from acidic pH environment (*cf.*, lysosome pH 3.5- 4, late endosome pH 5- 6, early endosome pH 6- 6.5) to neutral pH (cytosol pH=7-7.4), matches the endocytic route through the cell, where the pH change is used as a signal to release biomacromolecules, such as DNA. It confirms that the new cationic ChLCPs could act as an endosomolytic release system in gene therapy according to the hypothesis of "the proton sponge".

1. Introduction

The introduction of exogenous genetic material in cells is a key stage in the development of basic research in cellular biology. The term "transfection" is used to indicate the transfer of DNA into the nuclei of cells of higher organisms [1]. The development of *non-viral* DNA delivery vectors make it possible to model viral assembly and gene transfer by incorporating functional groups that enable particular assembly and transfer steps.

Cationic polymers (at physiological pH) are already used to condense anionic nucleic acids into nano-sized particle-like complexes called "polyplexes", through self-assembly driven by electrostatic interactions. By compressing DNA molecules to a relatively small size cellular internalization is facilitated and, thus, transfection efficacy is improved [2]. Whilst the intravascular route of



administration is an attractive approach for wide spread delivery, it is however particularly plagued by toxicity and biodistribution problems [3, 4]. New types of delivery vector are always welcome.

Several non-permanent polycations possessing substantial buffering capacity below physiological pH, such as lipopolyamines and polyethylenimines, are intrinsically efficient transfection agents, i.e. they do not need the addition of lysosomotropic bases, or cell targeting, or membrane disruption agents. These vectors have been shown to deliver genes as well as oligonucleotides both *in vitro* and *in vivo*. Their efficiency relies on extensive endosome swelling and rupture that provides an escape mechanism for the polycation/DNA polyplexes [5, 6]. The challenge, therefore, is to see if materials chemistry can provide more efficient, and ‘smart’, delivery vectors. One promising area of research uses liquid crystals (LCs).

Liquid crystals are self-organizing systems that form intermediate mesophases, combining the order of perfect crystals with the mobility of fluids [7]. These mesophases may be formed either by the effect of temperature (thermotropic) or of solvent concentration (lyotropic). Lyotropic liquid crystals, in the form of lipids, are of course ubiquitous throughout the life sciences [8]. They are a prerequisite for the development of life and the ability of cells to function.

In all LCs the longitudinal molecular axes are aligned parallel to each other, with the distribution of the molecular centres determining the type of LC. The most common types are the nematic (centres distributed isotropically), figure 1a, and smectic (where they are arranged in layers), figure 1b. Less common are the cholesteric, figure 1c, where nematic ordering is stacked in a superhelical structure, with a certain pitch, figure 1d. It is these LCs that are the focus of this paper.

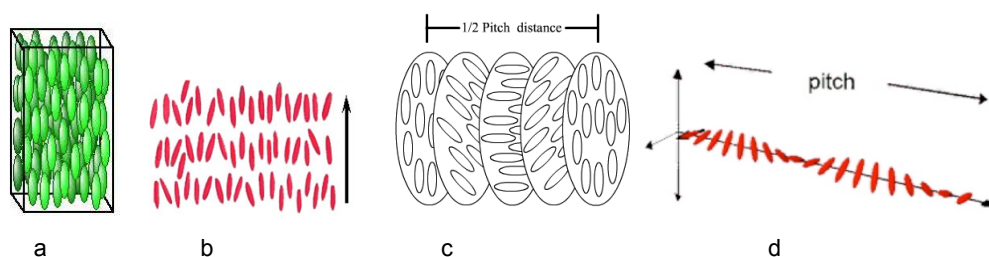


Figure 1. Liquid Crystal mesophases. (a) Nematic, (b) Smectic, (c, d) Cholesteric

Cholesteric liquid-crystal polymers (ChLCP), designated PTOBDME $[C_{34}H_{36}O_8]_n$ with the monomeric chemical formula shown in figure 2, and PTOBEE $[C_{26}H_{20}O_8]_n$ having the same mesogenic rigid group along the main chain but different side chain length, have been synthesised in our laboratory, through a stereoselective polycondensation reaction [9, 10]. The amphiphilic nature of the monomers makes them polymerize into helical chains.

These ChLCP have been extensively characterized [11]. They are both thermotropic and lyotropic, and adopt different conformations when dispersed in solution, depending on the solvent nature and concentration. They are also optically active and biocompatible against macrophages and fibroblast cellular lines, making them truly multifunctional materials.

We have previously shown that due to their lyotropic behaviour, these ChLCPs can entrap smaller molecules inside [12] and interact with liquid-crystalline biomacromolecules, such as nucleic acids and lipids (both neutral and cationic). The structures of the complexes formed have been previously studied by simultaneous synchrotron SAXS/WAXS [13, 14, 15].

Subsequently, formulations of the synthetic ChLCPs and cationic monomeric surfactants were developed in our lab to entrap an anionic plasmid of DNA. These complexes were successfully tested as non-viral vectors in gene therapy, both *in vitro* and *in vivo* [16, 17].

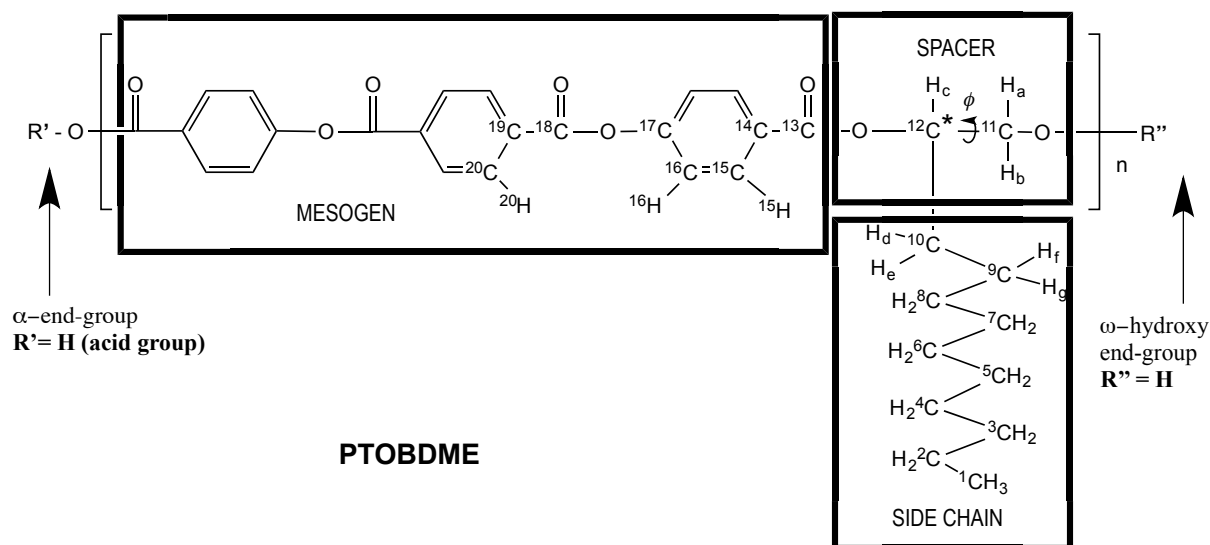


Figure 2. Chemical formula of PTOBDME $[C_{34}H_{36}O_8]_n$ subdivided into mesogen, spacer and side chain. PTOBEE $[C_{26}H_{20}O_8]_n$ shares the same mesogen and spacer but only has two carbon atoms in the side chain.

In order to specifically interact with complex polynucleotides, new *cationic* ChLCPs were synthesized, by functionalization of the precursors PTOBEE and PTOBDME with nitrogenated groups (NH_2 , choline, etc) [18]. The molecular model of Poly[PTOBEE] $_{10}$ - NH_2 is shown in figure 3.

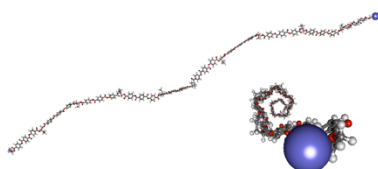


Figure 3. Molecular model of Poly[PTOBEE] $_{10}$ - NH_2 .
In the lower right sectional perspective view the terminal N atom of the amine end group is represented by a ball.

Polyplexes of the cationic ChLCP PTOBEE- NH_2 with the commercial anionic polynucleotide [Poly-C-Poly-G] have been studied by contrast variation small-angle neutron scattering (SANS), exploiting the difference in neutron scattering length densities (NSLD) of the two components ($1.887E+10/cm^2$ for PTOBEE- NH_2 , $3.320E+10/cm^2$ for [Poly-C-Poly-G]) to separately distinguish both component structures, and to highlight the whole polyplex, without any selective deuteration [19]. This provided complementary information to that obtained by SAXS [20].

In this paper SANS is used without contrast variation to investigate the pH-dependent conformational behaviour of three cationic ChLCPs. The pH value is a critical environmental parameter during transfection as it can be used as a signal to promote the efficient delivery of biomacromolecules or DNA to the correct intracellular compartment. The pH of an endosome is lower than that of the cytosol by up to two pH units, depending on the stage of endosomal development.

2. Experimental

Three cationic ChLCPs have been studied: PTOBDME-choline, PTOBDME- NH_2 , and PTOBEE- NH_2 . All samples were dispersed in aliquots of D_2O (to maximise the scattering contrast), pH-adjusted with

5M HCL or 5M NaOH (to match the conditions encountered during endocytic internalization; pH 3 to 7.4), at a fixed polymer concentration of 7 mg/ml. The pH's of the solutions were re-checked after dissolution of the polymers. In adjusting the pH, allowance was made for the small offset between pH and pD: $pD = pH + 0.4$.

Contrast variation (via adjusting D_2O/H_2O ratio) was not employed in this work, since the neutron scattering length densities (NSLD) of all the ChLCPs studied (between $1.3 - 3.3 \times 10^{10} \text{ cm}^{-2}$), are significantly different to that of D_2O (+6.3) to provide excellent contrast. As the SANS signal is proportional to the square of the difference in NSLD between the solute and solvent, using solvent mixtures with H_2O (-0.5 on the same scale) would have merely reduced the contrast. Contrast variation would, however, provide a means to elucidate individual contributions to the overall scattering in the polyplexes in future work.

SANS data were obtained on the LOQ small-angle diffractometer at the ISIS Pulsed Neutron Source (STFC Rutherford Appleton Laboratory, Didcot, U.K.) [21a, 21b]. This is a fixed-geometry "white beam" time-of-flight instrument which utilizes neutrons with wavelengths, λ , between 2 and 10 Å. Data are simultaneously recorded on two, two-dimensional, position-sensitive, neutron detectors, to provide a simultaneous Q ($=4\pi/\lambda \cdot \sin(\theta/2)$) range of $0.008 - 1.6 \text{ Å}^{-1}$, where θ is the scattering angle. Each polymer sample and corresponding solvent background was placed in 1 mm path length quartz disc-shaped cuvettes (volume 0.25 ml) and was measured for a total of 2 h in order to gather data of sufficient statistical precision. Each raw scattering data set was then corrected for the detector efficiencies, sample transmission and background scattering and converted to scattering cross-section data (denoted here as I vs Q) using the instrument-specific software [21c, 21d]. These data were placed on an absolute scale (cm^{-1}) using the scattering from a standard sample (a solid blend of hydrogenous and perdeuterated polystyrene) in accordance with established procedures [21e]. The data from the ChLCPs were analysed with a combination of partial Zimm plots (to extract the apparent radius-of-gyration of the nanostructure) [22] and Log-Log plots (*aka* Swollen Coil plots, to determine the fractal scaling of the nanostructure). The Zimm plots were fitted over the range $0.008 \leq Q \leq 0.02 \text{ Å}^{-1}$, whilst the Log-Log plots were fitted over a slightly extended range $0.008 \leq Q \leq 0.04 \text{ Å}^{-1}$.

3. Results and Discussion.

Figure 4 shows the small-angle neutron scattering (SANS) patterns, in $\log I(Q)$ versus Q representation, from cationic ChLCPs PTOBDME-Choline, PTOBDME- NH_2 and PTOBEE- NH_2 dispersed in D_2O at 7 mg/ml, as a function of pH (= 1.3, 3.58, 5.58, 7.2). These pH values were chosen to match the values in different cellular compartments (lysosome between pH 3.5 - 4, late endosome pH 5 - 6, early endosome pH 6 - 6.5 to cytosol, pH=7 - 7.4). Though superficially similar, there are some marked differences in both the intensity and Q -dependence of the scattering from the polymers as the pH changes, indicating that the size and/or shape of the solvated species is changing.

A zeroth-order approach to quantifying these changes is simply to determine the radius-of-gyration, R_g , of the ChLCPs from the SANS data. Traditionally this can be done through one of two low-angle linearisations, the Guinier plot or the Zimm plot [22]. We have used a variation of the latter as it has a slightly wider range of applicability (ie, is a little more robust to the presence of polydispersity). Whilst light scatterers will be familiar with the Zimm plot as a complex double extrapolation to infinite dilution and $Q=0$ (to correct for the strong angular dependence of the scattering), this is not actually necessary in order to estimate an apparent R_g as the slope of the Zimm plot, $1/I(Q)$ vs Q^2 , is just $(R_g^2/3) \times \text{intercept as } Q \rightarrow 0$, and SANS is always considered point scattering because the neutron wavelength is much larger than the object from which it is being scattered (the nucleus). The SANS data in Figure 4 are replotted in this partial Zimm representation (to denote that extrapolation to zero concentration was not performed) in Figure 5. Linearity is expected when $Q \cdot R_g < \pi$ (note: this is a slightly broader limit [23] than Zimm's original definition, which allows for the presence of some polydispersity). For R_g 's up to $\sim 200 \text{ Å}$ this would imply $0 < Q^2 < 0.00025 \text{ Å}^{-2}$. In some instances linearity would seem to extend beyond this range, in others a slight curve to the Zimm plot is evident

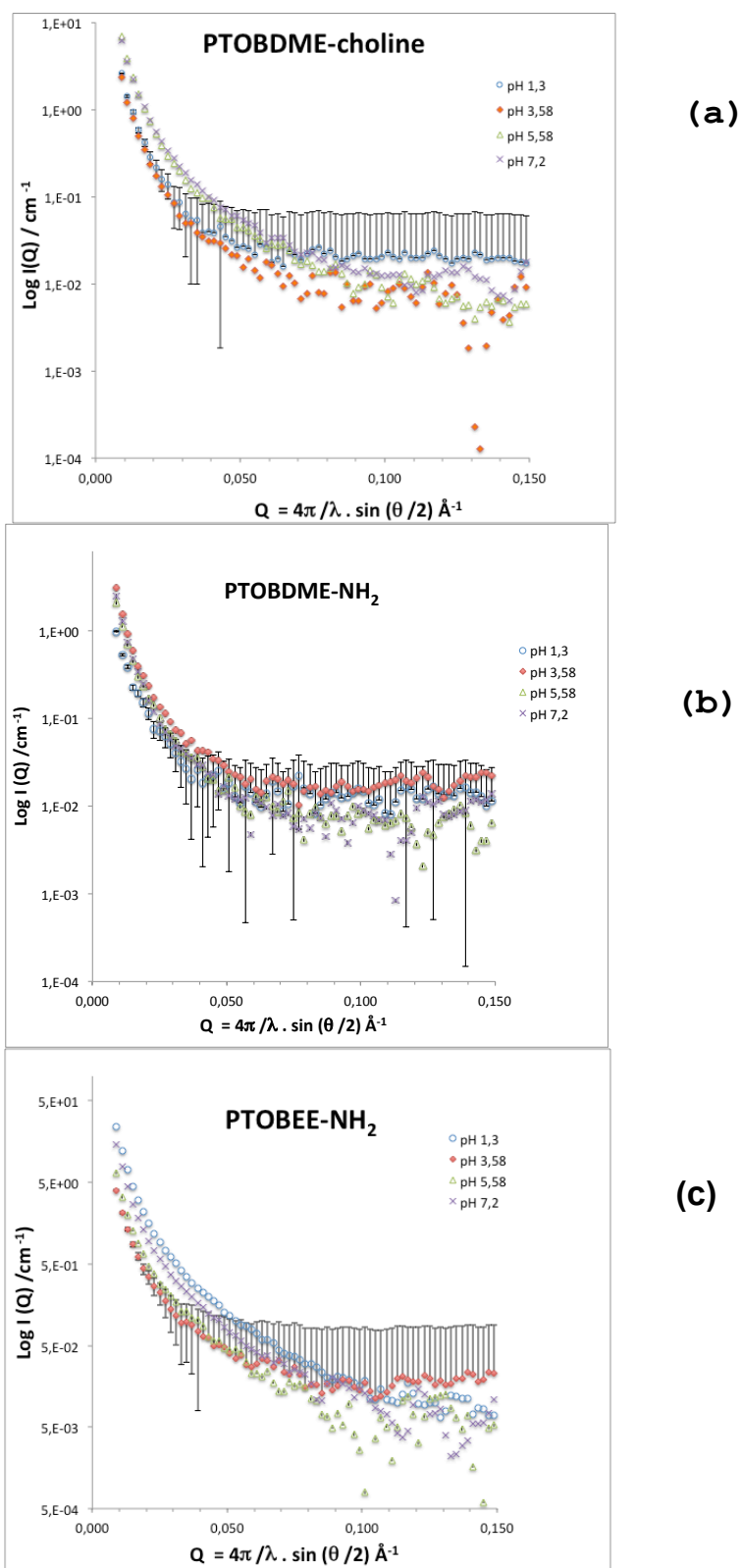


Figure 4. Small-angle neutron scattering patterns (SANS) of cationic ChLCPs, dispersed in D₂O at 7 mg/ml, as a function of pH: (a) PTOBDME-Choline; (b) PTOBDME-NH₂; (c) PTOBEE-NH₂.

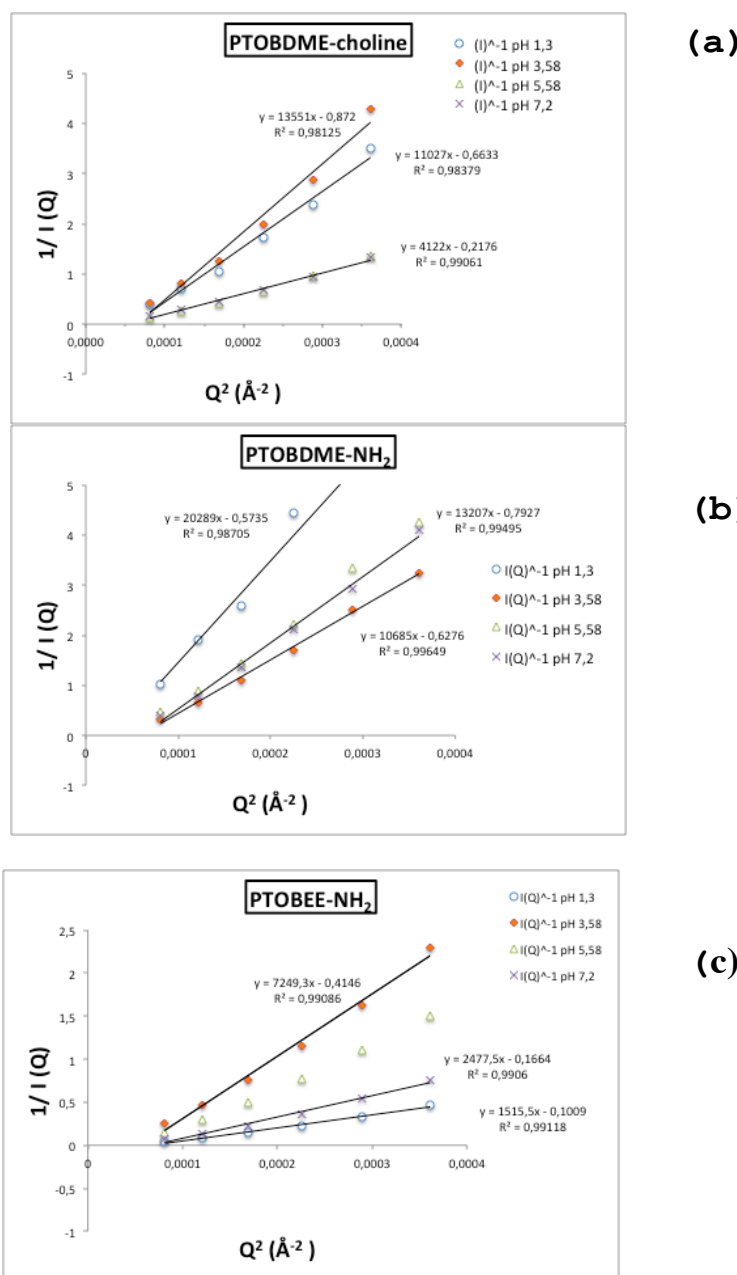


Figure 5. Partial Zimm plots of the cationic ChLCPs, dispersed in D₂O at 7 mg/ml, as a function of pH: (a) PTOBDME-Choline; (b) PTOBDME-NH₂; (c) PTOBEE-NH₂. The slope is proportional to $R_g^2/3$ at small Q .

suggesting that a more limited range might be more appropriate. But for consistency we report R_g 's determined over the same range of Q^2 .

In Figure 6 the apparent z-average radii of gyration, R_g , of the polymers extracted from the partial Zimm plots are displayed as a function of pH. With increasing pH, the apparent R_g of all the polymers increases up to a maximum value, before subsequently decreasing.

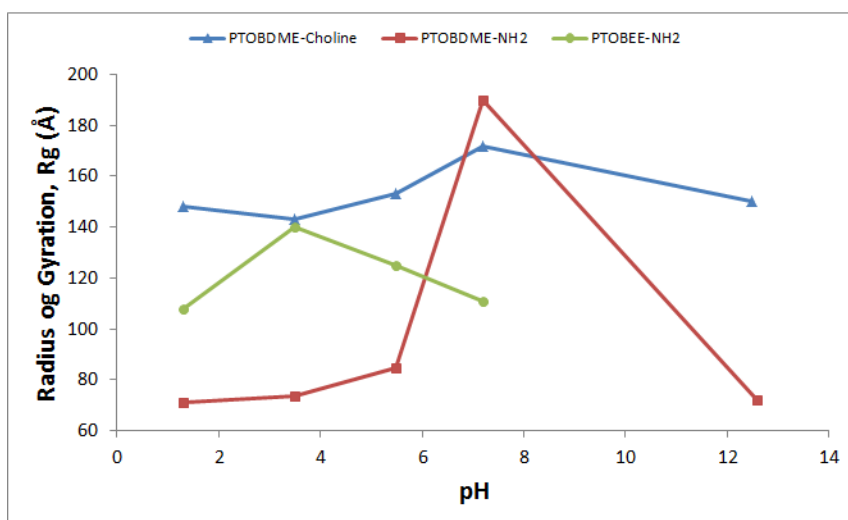


Figure 6. Variation of the apparent radius of gyration (\AA) of the cationic polymers dispersed in D_2O at $[7 \text{ mg/ml}]$ derived from the SANS data as a function of pH: (triangles) PTOBDME-Choline (squares) PTOBDME-NH₂ and (circles) PTOBEE-NH₂.

The cholesteric liquid crystalline nature of these new cationic polymers means they might reasonably be expected to have ‘less random coil’ solution conformations than other synthetic polymers, and there would seem to be evidence of this. In figure 7, the swollen coil fits to the SANS data from PTOBDME-NH₂ at pH 1.3 and pH 7.2 are shown. The gradients of the two linear regions are both significantly larger than what would be expected for an extended (filamentous) nanostructure, at -1.00, a ‘self-avoiding chain’ (ie, in a good solvent environment), at -1.66, or a ‘Gaussian chain’ (ie, in a theta solvent environment), at -2.00. Indeed the scaling displayed is more typical of some sort of network structure. The change observed in fractal scaling is also modest despite a large change in the apparent R_g (almost a factor of 3 for this polymer).

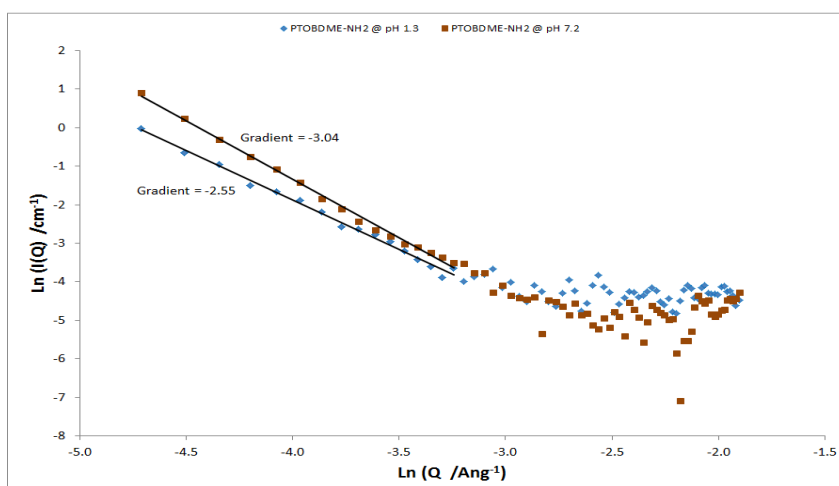


Figure 7. Swollen coil fits to the SANS from PTOBDME-NH₂ at pH 1.3 and pH 7.2. The gradients of the straight lines are -2.55 and -3.04, respectively.

The next best level of analysis would be to try and fit the SANS data to analytical descriptions of different shaped objects. We have tried this, using the well-known model-fitting program, FISH [28]. However we were unable to obtain a fit in which we had both confidence and belief that it represented physical reality. As an example, in Figure 8 fits of the SANS from PTOBDME-NH₂ at pH= 1,3 and 7,2 against a Debye Gaussian coil model are shown [29]. Neither calculation is a good description of the data; a not altogether surprising fact given the fractal scaling seen in Figure 7 but it illustrates the difficulties. The solution architecture of the ChLCPs is evidently quite challenging to determine. The analysis most likely to elucidate the structure is perhaps a MD simulation *constrained* against the experimental SANS data. We note that software packages to achieve this, explicitly accounting for solvent, are starting to become available [30].

The apparently large pH-induced change in apparent R_g (almost a factor of 3) for these ChLCP, on passing from acidic pH environment (*cf.* lysosome, endosome), towards neutral pH (*cf.* cytosol) and the posterior decrease in the more basic extreme, could be explained by the hypothesis of a molecular expansion up to a maximum, similar to the coil expansion described for other polymers at the same pH values [24], [25], [26]. The effect of extreme protonation/ deprotonation should be considered on intramolecular H-bridges (N-H...O) and on possible cleavage through ester groups, due to charge change.

The cleavage mechanism of a polyplex carrier, for delivery of a plasmid DNA, had been reported through S-S bonds when passing from pH 7 to 5.5 [27].

We have previously reported a decrease in the R_g of the precursor PTOBEE in both D₂O and in ethanol-d₆ when terminal amine groups are attached to form cationic PTOBEE-NH₂. This was ascribed to the presence of the nitrogen atoms affecting auto-aggregation, that is, a compaction of one molecule by the introduction of positive charges or by formation of H-bonds with the neighbouring oxygen atoms, or by a combination of the two [19]. The apparent R_g of PTOBEE-NH₂ calculated then (also from SANS data) at pH= 7, was 81 Å, assuming a rod-like nanostructure and 110 Å assuming a globular nanostructure. The latter figure is consistent with the value in Figure 5.

Work to better understand the origin of the pH-induced structural changes in these ChLCPs is in progress. However the results so far would seem to confirm the potential application of these new cationic ChLCP as endosomolytic polymers.

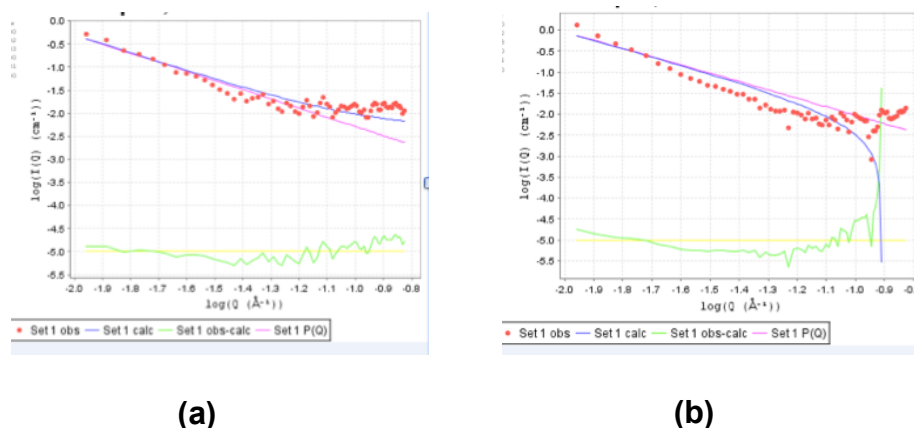


Figure 8. Debye Gaussian coil model fits to the SANS data from PTOBDME-NH₂ at pH 1,3 (a) and pH 7,2 (b). The red circles represent the experimental data, the blue line is the model calculation. The green line is the difference between the two, superimposed on a yellow abscissa. The fitting was conducted with the FISH program (see text).

4. Conclusions

The SANS patterns of synthetic cationic cholesteric liquid-crystal polymers PTOBDME-Choline, PTOBDME-NH₂ and PTOBEE-NH₂, dispersed in D₂O at 7 mg/ml, have been obtained at different pH values (= 1.3, 3.58, 5.58, 7.2), chosen to match the values in different cellular compartments (lysosome between pH 3.5 - 4, late endosome pH 5 - 6, early endosome pH 6 - 6.5 to cytosol, pH=7 - 7.4).

The apparent radius of gyration of the polymers, derived from the scattering data, proved to be highly sensitive to pH changes, initially increasing in size with increasing pH up to a maximum value, before subsequently decreasing once more at higher pH. The ChLCPs adopt rather different solution conformations to more conventional synthetic polymers, but the exact nature of the solution nanostructure and the explanation for the pH-sensitivity is, as yet, not fully understood.

The results shown here help indicate the potential of these new cationic ChLCPs as an endosomolytic release system in gene therapy, according to the hypothesis of "the proton sponge" where an endocytic pH change could be used as a signal to release a 'captive' biomacromolecule, such as DNA, in the correct intracellular compartment.

5. Acknowledgements

DR-M wishes to thank the MEC for a Scholarship of Specialization in International Organisms conducted at the ISIS Facility. STFC and ISIS are thanked for the provision of neutron beamtime.

6. References

- [1] Anderson WF 1998 Human gene therapy *Nature* **392** (6679 Suppl) (25-30).
- [2] Ibraheem D, Elaissari A, Fessi H Gene therapy and DNA delivery systems *Int J Pharm* 2014 **459**(1-2) 70-83.
- [3] Griffiths PC, Paul A, Khayat Z, Wan KW, King SM, Grillo I, Schweins R, Ferruti P, Franchini J, and Duncan R 2004 Understanding the Mechanism of Action of Poly(amidoamine)s as Endosomolytic Polymers: Correlation of Physicochemical and Biological Properties *Biomacromolecules* **5** 1422-1427.
- [4] Khayat Z, Griffiths PC, Grillo I, Heenan RK, King SM and Duncan R 2006 *Int. Journal of Pharmaceutics* **317** 175-186.
- [5] Von Gersdorff K, Sanders NN, Vandenbroucke R, De Smedt SC, Wagner E, Ogris M The internalization route resulting in successful gene expression depends on both cell line and polyethylenimine polyplex type *Mol Ther.* 2006 **14**(5) 745-53.
- [6] Behr, J P 1997 The Proton Sponge: a Trick to Enter Cells the Viruses Did Not Exploit *CHIMIA* **51** 34- 36.
- [7] a) de Gennes PG and Hebd CR 1975 Macromolecules and Liquid Crystals: Reflections on Certain Research *Seances Acad. Sci. Ser. B* **281** 101;
b) <http://plc.cwru.edu/tutorial/enhanced/files/lc/phase/phase.htm>
- [8] Ringsdorf H, Schlarb B, and Venzmer J 1988 Molecular Architecture and Function of Polymeric Oriented Systems: Models for the Study of Organization, Surface Recognition, and Dynamics of Biomembranes *Angew. Chem. Int. Ed. Engl.* **27** 113-158 ; c)
- [9] Pérez-Méndez M and Marco C 1997 New synthesis, thermal properties and texture of cholesteric poly[ethyl ethylene 4,4'-(terephthaloyldioxy)dibenzoate] *Acta Polymerica* **48**, 502-506.
- [10] Pérez-Méndez M and Marco Rocha C Preparing cholesteric liquid crystals - by adding acid di:chloride and butanediol to chloro-naphthalene, heating in nitrogen, decanting into toluene, etc Patent with n° EP1004650-A; WO9831771-A; WO9831771-A1; AU9854863-A; ES2125818-A1; ES2125818-B1; EP1004650-A1; US6165382-A; MX9906732-A1; JP2001513827-W; AU739076-B; EP1004650-B1; DE69824182-E.

- [11] Fayos J, Sánchez-Cortés S, Marco C and Pérez-Méndez M 2001 Conformational analysis and molecular modeling of cholesteric liquid-crystal polyesters based on XRD, Raman and transition thermal analysis *J. Macromol. Sci.-Physics* **B40**(3&4) 553-576.
- [12] Sanchez-Cortes S, López-Ramírez M, Pérez-Méndez M and Blanch G 2010 Trans-cis Isomerization of Carotenoid Lycopene upon Complexation with Cholesteric Polyester Carriers Investigated by Raman Spectroscopy and Density Functional Theory *Journal of Raman Spectroscopy* **41**, Issue 10, 1170-1177.
- [13] Pérez-Méndez M, Fayos J and Mateo CR 1999 Self-assembly of cholesteric liquid crystal polyesters and their stereoselective interaction with liposomes of DMPC *Advances in Biochirality* Elsevier Science S. A. Chapter 24.
- [14] Pérez-Méndez M, Areso S, Alarcón-Vaquero A, Elorza B and Malfois M 1998 Effect of polymer addition to lipid membranes as potential drug delivery systems. Structure and dynamics of their interaction *Annual Report EMBL* 372.
- [15] Pérez-Méndez M, Marsal-Berenguel R and Funari, SS 2003 Structural Characterization of the Interaction Between Cholesteric Liquid-Crystal Polymers and Molecules of Biological Interest *HASYLAB Annual Report* 11150.
- [16] Pérez Méndez M, Marsal Berenguel R and Sánchez-Cortés S 2003 New non-viral vectors based on biocompatible liquid-crystal polymers for the carriage and delivery of biomacromolecules and insoluble drugs as an strategy *Rev Oncol.* **4** Suppl 1 153.
- [17] Pérez-Méndez M, Fayos J, Blanch GP and Sanchez Cortes S 2011 Biofunctionalization of Cholesteric Liquid-Crystal Helical Polymers. Nanocarriers *ENCYCLOPEDIA OF NANOSCIENCE AND NANOTECHNOLOGY* **11** 547-580, Edited by H. S. Nalwa, ACS. American Scientific Publishers, ISBN: 1-58883-160-4
- [18] Pérez Méndez M Synthesis and characterization of new functionalized cholesteric liquid-crystalpolymers (to be published).
- [19] Pérez Méndez M and Hammouda B 2013 SAXS and SANS investigation of synthetic cholesteric liquid-crystal polymers for biomedical applications *Journal of Materials Science and Engineering* **B 3** (2) 104-115.
- [20] Perez Mendez M, Sanguino Otero J and Rodriguez Martinez D Structural characterization of cationic ChLCP/polynucleotide polyplexes by SAXS *To be published*
- [21] a) <http://www.isis.stfc.ac.uk/>
b) Heenan, RK, Penfold J, King SM. *J. Appl. Crystallogr.* 1997 **30** 1140.
c) Heenan RK, King SM, Osborn R, Stanley HB 1989 COLETTE Users Guide *Rutherford Appleton Laboratory Report RAL-89-128*, (1989)
d) King SM, Heenan RK 1995 Using COLETTE *Rutherford Appleton Laboratory Report RAL-95-005*.
e) Wignall GD, Bates FS 1987 *J. Appl. Crystallogr.* **20**, 28.
- [22] Zimm B H. The scattering of light and the radial distribution function of high polymer solutions *J. Chem. Phys.* 1948 **16** (12) 1093-1099 and 1099-1116.
- [23] Aho AV, Hopcroft JE, Ullman JD. Data Structures and Algorithms, Addison-Wesley Longman Publishing Co., Inc. Boston, MA, USA ©1983.
- [24] Benjaminsen RV, Matthebjerg MA, Henriksen JR, Moghimi SM, Andresen TL. The possible "proton sponge " effect of polyethylenimine (PEI) does not include change in lysosomal pH. *Mol. Ther.* 2013. **21**(1) 149-57.
- [25] Midoux P, Pichon C, Yaouanc J J and Jaffrès PA Chemical vectors for gene delivery: a current review on polymers, peptides and lipids containing histidine or imidazole as nucleic acids carriers *Br. J. Pharmacol* 2009 **157**(2) 166-78
- [26] Akinc A and Langer R Measuring the pH environment of DNA delivered using nonviral vectors: Implications for lysosomal trafficking 2002 *Biotechnology and Bioengineering* **78** 5 503-508.

- [27] Sanjoh M, Miyata K, Christie RJ, Ishii T, Maeda Y, Pittella F, Hiki S, Nishiyama N and Kataoka K. Dual Environment-Responsive Polyplex Carriers for Enhanced Intracellular Delivery of Plasmid DNA *Biomacromolecules* 2012, **13** (11) 3641–3649.
- [28] <http://www.diamond.ac.uk/Beamlines/Soft-Condensed-Matter/small-angle/SAXS-Software/CCP13/FISH.html>.
- [29] Debye P. Molecular-weight determination by light scattering, *Journal of Physical and Colloid Chemistry*, 1947, **51**, :18-32.
- [30] <http://www.ccpas.org>